

Exponentially Accelerated Sampling of Pauli Strings for Nonstabilizerness

Zhenyu Xiao^{1,*} and Shinsei Ryu²

¹*Princeton Quantum Initiative, Princeton University, Princeton, New Jersey 08544, USA*

²*Department of Physics, Princeton University, Princeton, New Jersey 08544, USA*

(Dated: January 5, 2026)

Quantum magic, quantified by nonstabilizerness, measures departures from stabilizer structure and underlies potential quantum speedups. We introduce an efficient classical algorithm that exactly computes stabilizer Rényi entropies and stabilizer nullity for generic many-body wavefunctions of N qubits. The method combines the fast Walsh-Hadamard transform with an exact partition of Pauli operators. It achieves an exponential speedup over direct approaches, reducing the average cost per sampled Pauli string from $\mathcal{O}(2^N)$ to $\mathcal{O}(N)$. Building on this framework, we further develop a Monte-Carlo estimator for stabilizer Rényi entropies together with a Clifford-based variance-reduction scheme that suppresses sampling fluctuations. We benchmark the accuracy and efficiency on ensembles of random magic states, and apply the method to random Clifford circuits with doped T gates, comparing different doping architectures. Our approach applies to arbitrary quantum states and provides quantitative access to magic resources both encoded in highly entangled states and generated by long-time nonequilibrium dynamics.

Introduction.— Quantum computers are exponentially faster than classical ones for certain computational tasks [1, 2]. Such quantum advantage relies on distinctive features of quantum states, including entanglement [3–6], yet entanglement alone is not sufficient. Clifford circuits acting on stabilizer states can generate extensive entanglement but still be efficiently simulated classically, as formalized by the Gottesman–Knill theorem [7, 8]. Therefore, genuine quantum speedup requires non-Clifford operations to generate non-stabilizer states. This motivates the notion of nonstabilizerness, also known as quantum magic [9–11]. It quantifies departures from stabilizer structure and, within a resource-theoretic viewpoint, characterizes the difficulty of preparing the state [11, 12]. Understanding how nonstabilizerness is generated and redistributed across different quantum dynamics [13–33] is important in quantum science and engineering.

Beyond its role as a computational resource, nonstabilizerness also quantifies many-body state complexity [14, 34–36], capturing information distinct from entanglement-based measures. Recent work has shown that magic-based diagnostics can diagnose ground-state phase transitions [37–39], reveal universal structures described by conformal field theory [40–43], and probe quantum chaos [44–48]. They can also offer additional insight into thermalization [18, 22, 49, 50], complementing entanglement entropy and out-of-time-order correlators [51]. However, quantifying nonstabilizerness typically involves nonlinear functionals of the many-body wave function and is therefore notoriously difficult in practice [14]. The challenge is particularly acute for generic long-time dynamics, where the evolving states commonly develop volume-law entanglement and admit no efficient classical compression.

There exist several measures of nonstabilizerness in quantum information theory, such as the robustness of

magic and the relative entropy of magic [10, 14, 52]. These quantities are defined through optimizations over operator decompositions, making direct numerical evaluation impractical beyond a few qubits. More recently, computable diagnostics based on the Pauli expansion, $P \in \{I, X, Y, Z\}^{\otimes N}$, have been introduced, including stabilizer Rényi entropies [53], stabilizer nullity [54, 55], and Bell magic [56]. While these Pauli-string-based measures avoid explicit optimizations, their numerical cost remains substantial. For a generic N -qubit state $|\psi\rangle$ represented as a full state vector, evaluating a single correlator $\langle\psi|P|\psi\rangle$ requires $\mathcal{O}(2^N)$ time. Consequently, a brute-force evaluation that enumerates all 2^{2N} Pauli strings scales as $\mathcal{O}(2^{3N})$.

This difficulty is alleviated when the state admits an efficient classical representation [57, 58]. For a matrix product state (MPS) with bond dimension χ , exact evaluation of the α -order ($\alpha \geq 2$) stabilizer Rényi entropy scales as $\mathcal{O}(N\chi^{6\alpha})$ [59], and can be reduced to $\mathcal{O}(N\chi^4)$ [60] using truncated “replica MPS” constructions. However, these techniques become inefficient for long-time dynamics, where generic states develop volume-law entanglement, and the required bond dimension grows exponentially with system size. Monte Carlo sampling over Pauli strings provides an alternative approach [45]. With \mathcal{N} samples, the cost is $\mathcal{O}(\mathcal{N}2^N)$ for full state vectors and $\mathcal{O}(\mathcal{N}\mathcal{N}\chi^3)$ for MPS [61]. In practice, sampling can remain difficult when the Pauli-weight distribution is strongly inhomogeneous, where \mathcal{N} may need to grow exponentially with N . Finally, efficient specialized methods exist for restricted families of states, including free-fermion states [62, 63] and sign-problem-free quantum spin models [64, 65], but efficient approaches applicable to generic many-body states remain limited.

In this Letter, we develop an efficient classical framework for computing Pauli-string-based measures of nonstabilizerness for generic N -qubit wavefunctions. The

framework partitions Pauli operators into 2^N families $\{P_{x,z}\}_{z \in \mathbb{F}_2^N}$ and evaluates all correlators within each family simultaneously via a fast Walsh-Hadamard transform [66]. As a result, the cost of obtaining stabilizer Rényi entropy and stabilizer nullity is reduced from brute-force $\mathcal{O}(2^{3N})$ to $\mathcal{O}(N2^{2N})$. Building on this structure, we introduce a Monte Carlo estimator together with a Clifford preconditioning step that significantly suppresses sampling fluctuations. We benchmark both the exact and Monte-Carlo variants on ensembles of random magic states. We then use the method to address a question of magic generation: for a fixed budget of nonstabilizerness resources, which circuit architecture increases stabilizer Rényi entropy more efficiently?

Stabilizer Rényi entropy and stabilizer nullity.— We consider an N -qubit pure state $|\psi\rangle$ with $d = 2^N$. Expanding the density matrix in the Pauli basis $P \in \{I, X, Y, Z\}^{\otimes N}$, we write $|\psi\rangle\langle\psi| = \sum_P \frac{1}{\sqrt{d}} c_P P$ with $c_P = \langle\psi|P|\psi\rangle$. Using Pauli orthogonality and $\text{Tr}[(|\psi\rangle\langle\psi|)^2] = 1$, one has $\sum_P \frac{1}{d} |c_P|^2 = 1$, so $\{\frac{1}{d} |c_P|^2\}$ defines a probability distribution over Pauli strings. The stabilizer Rényi entropy is the Rényi entropy of this distribution (shifted by N) [53],

$$M_\alpha(|\psi\rangle) := \frac{1}{1-\alpha} \log_2 \left(\sum_P \frac{|c_P|^{2\alpha}}{d^\alpha} \right) - N. \quad (1)$$

The stabilizer nullity [54, 55] is defined by

$$\nu(|\psi\rangle) := N - \log_2 |\text{STAB}(|\psi\rangle)|, \quad (2)$$

where $\text{STAB}(|\psi\rangle)$ denotes the stabilizer group of $|\psi\rangle$ and $|\text{STAB}(|\psi\rangle)|$ counts Pauli strings P satisfying $P|\psi\rangle = \pm|\psi\rangle$. Both $M_\alpha(|\psi\rangle)$ and $\nu(|\psi\rangle)$ are non-negative, vanish if and only if $|\psi\rangle$ is a stabilizer state, and are invariant under Clifford operations [53]. In magic-state resource theory, M_α is not a monotone for $\alpha < 2$ [67], whereas M_α for $\alpha > 2$ and ν are monotones under stabilizer operations [68].

Fast Walsh-Hadamard Pauli sampling.— To obtain numerically exact values of $M_\alpha(|\psi\rangle)$ or $\nu(|\psi\rangle)$ by brute-force Pauli enumeration, one would in general need all d^2 correlators $\langle\psi|P|\psi\rangle$. We first illustrate the key idea by restricting to Pauli strings containing only I and Z : $P_z := Z^{z_1} \otimes Z^{z_2} \otimes \cdots \otimes Z^{z_N}$ with $z_i \in \{0, 1\}$ and $z = (z_1, \dots, z_N) \in \mathbb{F}_2^N$. Writing $|\psi\rangle = \sum_{b \in \mathbb{F}_2^N} \psi(b)|b\rangle$, we have $P_z|b\rangle = (-1)^{z \cdot b}|b\rangle$ with $z \cdot b := \sum_i z_i b_i$ (using $Z|0\rangle = |0\rangle$ and $Z|1\rangle = -|1\rangle$), and hence

$$\langle\psi|P_z|\psi\rangle = \sum_{b \in \mathbb{F}_2^N} (-1)^{z \cdot b} |\psi(b)|^2, \quad (3)$$

which is precisely the discrete Fourier transform on $(\mathbb{F}_2)^N$ (Walsh-Hadamard transform) of $f(b) := |\psi(b)|^2$ [69]. Computing all $\{\langle\psi|P_z|\psi\rangle\}_z$ by brute force costs $\mathcal{O}(2^{2N})$, whereas the fast Walsh-Hadamard transform (FWHT)

evaluates the full transform in $\mathcal{O}(N2^N)$ time via a hierarchy of pairwise sum-difference updates [66]. The FWHT can be viewed as iteratively applying the Hadamard gate $H = \frac{1}{\sqrt{2}} \begin{pmatrix} 1 & 1 \\ 1 & -1 \end{pmatrix}$ to the length- 2^N vector $|f\rangle := \sum_{b \in \mathbb{F}_2^N} f(b)|b\rangle$. Applying $\sqrt{2}H$ to the first qubit yields

$$(\sqrt{2}H \otimes I^{\otimes(N-1)})|f\rangle = \sum_{z_1, b_1} \left(\sum_{b_1 \in \mathbb{F}_2} (-1)^{z_1 b_1} f(b_1, b_{\bar{1}}) \right) |z_1, b_{\bar{1}}\rangle, \quad (4)$$

with $b = (b_1, b_{\bar{1}})$. This step is the \mathbb{F}_2 Fourier transform on the first index of $f(b_1, b_{\bar{1}})$. Iterating over all qubits yields $(\sqrt{2}H)^{\otimes N}|f\rangle = \sum_{z \in \mathbb{F}_2^N} \langle\psi|P_z|\psi\rangle |z\rangle$, so $\{\langle\psi|P_z|\psi\rangle\}_z$ are read off from the amplitudes. Each application of $\sqrt{2}H$ performs $\mathcal{O}(2^N)$ floating-point operations, giving an overall time complexity of $\mathcal{O}(N2^N)$.

Algorithm 1 Fast Walsh–Hadamard Pauli sampling

Input: An N -qubit wave function $|\psi\rangle = \sum_{b \in \mathbb{F}_2^N} \psi(b)|b\rangle$ and numerical tolerance ϵ (for stabilizer nullity).
Output: Stabilizer Rényi entropy M_α and stabilizer nullity ν .

```

1: Initialize  $m_\alpha \leftarrow 0$ ,  $\nu_{\text{cnt}} \leftarrow 0$ .
2: for  $x \in \mathbb{F}_2^N$  do
3:   Define  $f_x(b) \leftarrow \overline{\psi(b)} \psi(b \oplus x)$  for all  $b \in \mathbb{F}_2^N$ .
4:   Compute the FWHT  $F_x(z) \leftarrow \sum_{b \in \mathbb{F}_2^N} (-1)^{z \cdot b} f_x(b)$  for
   all  $z \in \mathbb{F}_2^N$ .
5:    $\nu_x \leftarrow \#\{z \in \mathbb{F}_2^N : |F_x(z)| - 1| < \epsilon\}$ .
6:    $m_{\alpha;x} \leftarrow \sum_{z \in \mathbb{F}_2^N} |F_x(z)|^{2\alpha} / 2^{N\alpha}$ .
7:    $m_\alpha \leftarrow m_\alpha + m_{\alpha;x}$ ;  $\nu_{\text{cnt}} \leftarrow \nu_{\text{cnt}} + \nu_x$ .
8: end for
9: return  $M_\alpha = \frac{1}{1-\alpha} \log_2(m_\alpha) - N$ ,  $\nu = N - \log_2(\nu_{\text{cnt}})$ .

```

To generalize this idea to arbitrary Pauli strings, we use the standard binary labeling: any N -qubit Pauli can be written (up to an overall phase) as a product of X and Z operators, and is specified by a pair $(x, z) \in \mathbb{F}_2^N \times \mathbb{F}_2^N$ [6, 8],

$$P_{x,z} = e^{i\phi(x,z)} X^x Z^z, \quad X^x := \bigotimes_{j=1}^N X_j^{x_j}, \quad Z^z := \bigotimes_{j=1}^N Z_j^{z_j}, \quad (5)$$

where $e^{i\phi(x,z)}$ is a phase convention and does not affect $|\langle\psi|P_{x,z}|\psi\rangle|$. In the computational basis $\{|b\rangle\}_{b \in \mathbb{F}_2^N}$, X^x acts as a bit flip, $X^x|b\rangle = |b \oplus x\rangle$, while $Z^z|b\rangle = (-1)^{z \cdot b}|b\rangle$ with $z \cdot b := \sum_i z_i b_i$. Therefore, for $|\psi\rangle = \sum_b \psi(b)|b\rangle$,

$$\langle\psi|P_{x,z}|\psi\rangle = e^{i\phi(x,z)} \sum_{b \in \mathbb{F}_2^N} \overline{\psi(b)} (-1)^{z \cdot b} \psi(b \oplus x). \quad (6)$$

For each fixed x , define $f_x(b) := \overline{\psi(b)} \psi(b \oplus x)$. Equation (6) is exactly the Walsh-Hadamard transform of f_x from b -space to z -space, so a single FWHT produces $\{\langle\psi|P_{x,z}|\psi\rangle\}_{z \in \mathbb{F}_2^N}$ in $\mathcal{O}(N2^N)$ time. Sweeping x over \mathbb{F}_2^N

enumerates the expectation values of all 4^N Pauli strings, for a total cost of 2^N FWHTs, i.e. $\mathcal{O}(N2^{2N})$ time complexity. This yields an exponential speedup compared to brute-force enumeration, which scales as $\mathcal{O}(2^{3N})$ when each correlator is evaluated in $\mathcal{O}(2^N)$ time.

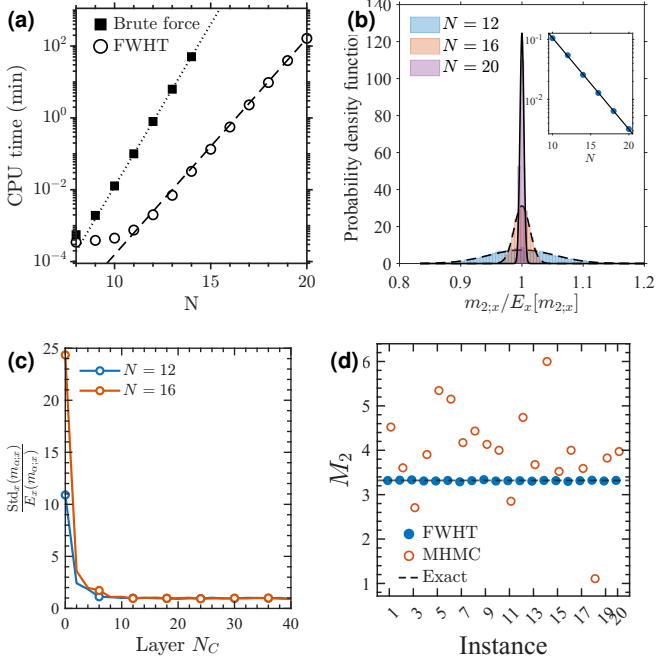


FIG. 1. (a) Runtime for computing M_2 of random magic states by brute-force versus FWHT-based Pauli enumeration; dashed lines indicate $\sim \mathcal{O}(2^{3N})$ and $\sim \mathcal{O}(2^{2N})$ scaling. (b) Probability density of the normalized partial moment $m_{2;x}/E_x[m_{2;x}]$ for Haar-random states (black: Gaussian fits); inset shows $\text{Std}_x(m_{2;x})/\mathbb{E}_x(m_{2;x})$ as a function of N . (c) Normalized standard deviation $\text{Std}_x(m_{2;x})/\mathbb{E}_x(m_{2;x})$ versus Clifford depth N_C for $|\psi_m\rangle = |T\rangle^{\otimes N_T} \otimes |0\rangle^{\otimes (N-N_T)}$ at several N . (d) Fluctuations of M_2 estimates for highly entangled $C|\psi_m\rangle$ at $N = 16$: MC+FWHT (sampling $\{P_{x,z}\}_z$ with $\mathcal{N} = 10^4$) versus Metropolis–Hastings sampling of Pauli strings (1.6×10^6 samples). The Metropolis–Hastings data use $10\times$ more CPU time.

To compute the stabilizer Rényi entropy, after each FWHT, we accumulate the partial 2α -order moment $m_{\alpha;x} := \sum_{z \in \mathbb{F}_2^N} |\langle \psi | P_{x,z} | \psi \rangle|^{2\alpha} / d^\alpha$, and hence $M_\alpha(|\psi\rangle) = \frac{1}{1-\alpha} \log_2 (\sum_x m_{\alpha;x}) - N$. For the stabilizer nullity, it suffices to count the number of Pauli strings with $|\langle \psi | P_{x,z} | \psi \rangle| \approx 1$ (within a numerical tolerance, e.g. 10^{-7}), since for pure states $|\langle \psi | P | \psi \rangle| = 1$ implies $P|\psi\rangle = \pm|\psi\rangle$. This algorithm is summarized in Algorithm 1. We benchmark the FWHT algorithm against brute-force Pauli enumeration on highly entangled random magic states (see definition later). Both approaches agree with the analytic values up to numerical round-off, while the FWHT method is markedly faster, consistent with the expected scalings $\mathcal{O}(N2^{2N})$ versus $\mathcal{O}(2^{3N})$ [Fig. 1(a)].

Monte-Carlo sampling with FWHT.— We can approximate M_α by Monte-Carlo (MC) sampling over $x \in \mathbb{F}_2^N$

rather than sweeping all $d = 2^N$ values. Specifically, we choose $\mathcal{N} < d$ distinct values of x uniformly at random, compute $\{\langle \psi | P_{x,z} | \psi \rangle\}_{z \in \mathbb{F}_2^N}$ via one FWHT for each sampled x , and accumulate the partial moment $m_{\alpha;x}$. This yields the unbiased estimator

$$\hat{S} := \frac{d}{\mathcal{N}} \sum_{x \in \text{MC}} m_{\alpha;x}, \quad S := \sum_{x \in \mathbb{F}_2^N} m_{\alpha;x}. \quad (7)$$

(We apply special treatment on the identity Pauli string [70].) Notably, this procedure produces $\mathcal{N}2^N$ Pauli correlators at total cost $\mathcal{O}(\mathcal{N}2^N)$, i.e., an average cost $\mathcal{O}(N)$ per sampled Pauli string, compared to $\mathcal{O}(2^N)$ for direct evaluation of a single correlator $\langle \psi | P | \psi \rangle$.

The efficiency of this MC scheme is controlled by fluctuations of $m_{\alpha;x}$ over x . Sampling uniformly over x with $\mathcal{N} \ll d$, the relative standard deviation obeys

$$\frac{\sigma_{\hat{S}}}{S} \approx \frac{1}{\sqrt{\mathcal{N}}} \frac{\text{Std}_x(m_{\alpha;x})}{\mathbb{E}_x(m_{\alpha;x})}, \quad (8)$$

where $\mathbb{E}_x[\cdot]$ and $\text{Std}_x(\cdot)$ denote the mean and standard deviation under uniform $x \in \mathbb{F}_2^N$. As $M_\alpha = \frac{1}{1-\alpha} \log_2 S - N$, we have

$$\sigma_{\hat{M}_\alpha} \approx \frac{\text{Std}_x(m_{\alpha;x})}{|1-\alpha| \ln 2 \sqrt{\mathcal{N}} \mathbb{E}_x(m_{\alpha;x})}. \quad (9)$$

The x -landscape standard deviation $\text{Std}_x(m_{\alpha;x})$ determines the efficiency of MC sampling.

We first consider Haar-random pure states and focus on $\alpha = 2$. Numerically, we find that $m_{2;x}$ is well described by a Gaussian distribution and that $\text{Std}_x(m_{2;x})/\mathbb{E}_x(m_{2;x})$ decreases exponentially with respect to N [see Fig. 1(b)], so that only a small \mathcal{N} is needed to accurately estimate M_2 . For example, with $\mathcal{N} = 10$ samples at $N = 24$ we obtain $M_2 = 21.9999(2)$, in excellent agreement with the exact Haar value $M_2^{\text{Haar}} = \log_2(2^N + 3) - 2 \approx 22$ [45].

We next study states with a much more inhomogeneous x landscape. Consider the product state $|\psi_m\rangle = |T\rangle^{\otimes N_T} \otimes |0\rangle^{\otimes (N-N_T)}$, where $|T\rangle = \frac{1}{\sqrt{2}}(|0\rangle + e^{i\pi/4}|1\rangle)$ and $N_T = \lfloor N/2 \rfloor$. This state has $\nu = N_T$ and $M_2 = N_T \log_2(4/3)$, much smaller than the Haar-typical value $M_2 \approx N - 2$ at the same N [45, 53]. Consistent with low M_2 , we observe a significantly larger $\text{Std}_x(m_{2;x})$ [see Fig. 1(c)], and naive MC requires substantially larger \mathcal{N} to reach a comparable accuracy. This difficulty is compounded by the fact that, for each fixed x , the family $\{P_{x,z}\}_{z \in \mathbb{F}_2^N}$ forms a highly-structured slice of Pauli space: for example, $\{P_{0,z}\}_{z \in \mathbb{F}_2^N}$ contains only I/Z strings and therefore overrepresents small-support operators, whereas for $x = 11 \cdots 1$ the family $\{P_{x,z}\}_z$ contains only full-support strings. As a result, uniform sampling over x can oversample particular support sectors.

Clifford preconditioning for MC sampling.— A practical variance-reduction step is to apply a random Clifford unitary C to scramble Pauli weights before sampling.

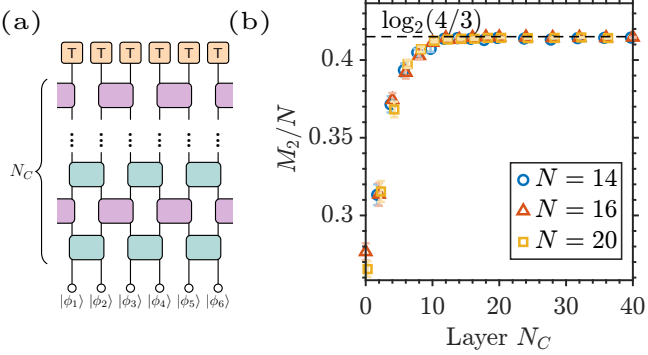


FIG. 2. (a) Quantum circuit begin with a N -qubit random Clifford product state, followed by N_C layers of random two-qubit Clifford gates and T gates on all qubits. (b) Stabilizer Rényi entropy density M_2/N of the left-figure state as a function of N_C for different system sizes N . The data are averaged over 80 random instances. For $N = 14, 16$, we use the exact FWHT algorithm; for $N = 20$, the number of Monte Carlo samples is $\mathcal{N} = 2 \times 10^4$.

Concretely, we take \mathcal{C} to be a random brick-wall circuit, with each two-qubit gate drawn uniformly from the two-qubit Clifford group \mathcal{C}_2 ($|\mathcal{C}_2| = 11520$) [71]. We then perform the same MC+FWHT procedure on $\mathcal{C}|\psi\rangle$; since M_α is invariant under Clifford operations, $M_\alpha(\mathcal{C}|\psi_m\rangle) = M_\alpha(|\psi_m\rangle)$. As shown in Fig. 1(c), $\text{Std}_x(m_{2;x})$ decreases rapidly with the Clifford depth N_C and reaches a plateau, and the plateau value is almost independent of system size N for the state $|\psi_m\rangle$. In our numerics, a depth $N_C \simeq 2N$ is sufficient to reach this plateau across the system sizes studied. We therefore believe that for generic N -qubit states, a depth $N_C = O(N)$ typically suffices, since random brick-wall Clifford circuits generate volume-law entanglement [72] and spread Pauli support across the system [73]. With this Clifford preconditioning, a moderate \mathcal{N} already yields accurate estimates of M_2 for $|\psi_m\rangle$ [see Fig. 1(d)]. Notably, the complexity of Clifford preconditioning with depth $N_C = O(N)$ costs $\mathcal{O}(N^2 2^L)$, which is generally lower than the time complexity $\mathcal{O}(\mathcal{N} N 2^N)$ for MC sampling.

Finally, we comment on the previously widely used approach of direct Pauli-string sampling with Metropolis-Hastings updates [45, 74, 75]. For states with low nonstabilizerness but high entanglement, such as $\mathcal{C}|\psi_m\rangle$ at large N_C , this method can become inefficient. Low nonstabilizerness typically entails a strongly inhomogeneous Pauli-weight distribution, and in highly entangled states, the dominant-weight strings need not be connected by local moves in Pauli space. As a result, Metropolis-Hastings updates can have very small acceptance ratios; for $\mathcal{C}|\psi_m\rangle$ we find an acceptance ratio of ≈ 0.03 . Even with ten times more computational budget, we observe substantially larger fluctuations than in the MC+FWHT approach [Fig. 1(d)], consistent with the combination of low acceptance and the $\mathcal{O}(2^N)$ cost of evaluating a sin-

gle correlator $\langle \psi | P | \psi \rangle$ in direct sampling, compared to an average $\mathcal{O}(N)$ cost per sampled Pauli string in our FWHT-based scheme.

Doping architectures of T gates.— We study how the ability of $T = \begin{pmatrix} 1 & 0 \\ 0 & e^{i\pi/4} \end{pmatrix}$ gates to generate nonstabilizerness [15, 16, 68, 76–79] depends on the entanglement structure of the underlying stabilizer state [26]. We begin with a random product stabilizer state $\bigotimes_{i=1}^N |\phi_i\rangle$, where each $|\phi_i\rangle$ is drawn uniformly from the six single-qubit Clifford states (eigenstates of X , Y , and Z). We apply N_C layers of random two-qubit Clifford gates in a brick-wall pattern to obtain an entangled stabilizer state $|\psi(N_C)\rangle$. Before saturation, its bipartite entanglement entropy grows approximately linearly with N_C . To generate extensive nonstabilizerness, we apply T on every qubit and evaluate M_2 for $T^{\otimes N}|\psi(N_C)\rangle$ [Fig. 2(a)]. We find that the ensemble-averaged density $\mathbb{E}[M_2/N]$ increases with the number of Clifford layers N_C and saturates at large N_C . Moreover, for $N \geq 14$ the data for different N nearly collapse when plotted as a function of N_C [Fig. 2(b)], indicating that the crossover depth to saturation depends only weakly on N over the accessible system sizes. The limiting values can be obtained analytically. At $N_C = 0$, additivity gives $M_2(\bigotimes_{i=1}^N T|\phi_i\rangle) = \sum_{i=1}^N M_2(T|\phi_i\rangle)$ [53]. If $|\phi_i\rangle$ is a Z eigenstate (probability 1/3), then $T|\phi_i\rangle$ remains a stabilizer state and $M_2(T|\phi_i\rangle) = 0$; otherwise $M_2(T|\phi_i\rangle) = \log_2(4/3)$ [Eq. (1)]. Therefore, $\mathbb{E}[M_2/N] = \frac{2}{3} \log_2(4/3)$. In the opposite limit of large N_C , we approximate the Clifford circuit by a uniform distribution over the Clifford group; using standard Clifford averaging techniques, we obtain $\mathbb{E}[M_2/N] = \log_2(4/3) + \mathcal{O}(2^{-N})$ [70], consistent with the numerical plateau.

A single-shot application of T gates to all qubits can generate extensive non-stabilizerness. However, even the saturation value $\mathbb{E}[M_2/N] \approx \log_2(4/3) \approx 0.415$ for a large number N_C of Clifford layers is far below the density of a Haar random state, which approaches 1 for large N [45]. To further increase nonstabilizerness, we repeat the procedures: N_C layers of random two-qubit Clifford gates, followed by $T^{\otimes N}$. We find that $\mathbb{E}[M_2]$ increases with the number of T -doping cycles and approaches M_2^{Haar} after several scramble- T -gate injection steps; the gap $M_2^{\text{Haar}} - \mathbb{E}[M_2]$ decays exponentially with respect to the steps, and larger N_C implies larger decay rates [Fig. 3(a)].

The results above indicate that, at a fixed T budget, stronger scrambling between injections (i.e., more layers of random two-qubit Clifford dynamics) enhances the growth of nonstabilizerness. We next ask a complementary question: at a fixed injection rate (i.e., a fixed ratio between the number of random Clifford layers and the number of injected T gates), which dynamical architecture produces nonstabilizerness more efficiently? In particular, is it preferable to inject T gates in tempo-

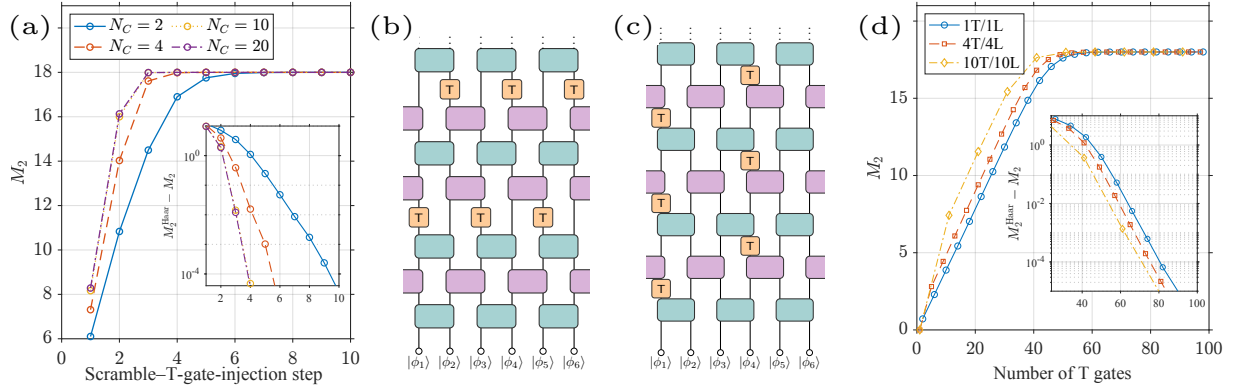


FIG. 3. (a) Ensemble-averaged M_2 versus the number of scramble- T -injection cycles for different numbers N_C of random two-qubit Clifford layers per cycle. Inset: the gap $M_2^{\text{Haar}} - \mathbb{E}[M_2]$ on a logarithmic scale. (b, c) Two T -doping architectures at fixed injection rate (one T gate per Clifford layer on average), illustrated for $N = 6$: (b) bursty injection with $N_B = N/2 = 3$ parallel T gates applied after $N_B = 3$ Clifford layers; (c) uniform injection with T gates spread among the Clifford layers ($N_B = 1$). (d) $\mathbb{E}[M_2]$ versus the total number of injected T gates for several block sizes N_B . Labels such as “10T/10L” denote blocks of 10 T gates applied after 10 Clifford layers (and similarly for “4T/4L” and “1T/1L”). Inset: $M_2^{\text{Haar}} - \mathbb{E}[M_2]$ on a logarithmic scale. Parameters: $N = 20$, MC sample size $\mathcal{N} = 2 \times 10^5$, and 80 circuit realizations per data point.

rally concentrated “bursts” or to distribute them more uniformly throughout the evolution?

To address this, we consider protocols in which the total number of injected T gates equals the total number of Clifford layers, i.e., one T gate per Clifford layer on average. We parameterize the architecture by a block size $N_B \leq N$. Each cycle consists of N_B layers of random brick-wall Clifford gates followed by a layer of N_B parallel T gates, and the cycle is repeated. Within each T -injection layer, the N_B qubits are chosen to be (approximately) equally spaced to suppress short-range interference between simultaneously injected T gates; successive injection layers are arranged in a staggered pattern to suppress temporal interference [Fig. 3 (b,c)]. We find that larger block sizes N_B yield systematically larger $\mathbb{E}[M_2]$ at a fixed total number of injected T gates. Quantitatively, in both architectures, the gap to the Haar benchmark, $M_2^{\text{Haar}} - \mathbb{E}[M_2]$, decays exponentially with the total number of injected T gates [Fig. 3 (d)], with similar decay rates across N_B . Nevertheless, for the same T budget, bursty protocols (larger N_B) achieve a smaller residual gap, i.e., a higher nonstabilizerness [Fig. 3 (d)].

Summary and outlook.— We introduced an FWHT-based framework for evaluating stabilizer Rényi entropies and stabilizer nullity of generic N -qubit wavefunctions, and developed an efficient Monte Carlo variant with Clifford preconditioning. This reduces the average cost per sampled Pauli string from $\mathcal{O}(2^N)$ to $\mathcal{O}(N)$. Because the method operates directly on full wavefunctions, it remains applicable even for volume-law-entangled states. This opens a quantitative route to studying magic in regimes where entanglement is already extensive but non-Clifford resources are scarce. From this perspective, our analysis of T -doping architectures in random Clifford circuits provides a concrete benchmark for compar-

ing circuit-level strategies to generate, redistribute nonstabilizerness under realistic resource constraints. More broadly, it would be interesting to apply the framework to nonequilibrium many-body problems, for example, to track how conserved quantities [49, 80–82] and dynamical constraints [83] influence the growth of nonstabilizerness and its interplay with entanglement during thermalization.

Finally, a direct extension is to subsystem (mixed-state) stabilizer Rényi entropies (see Supplemental Materials [70]), and it would be interesting to apply the framework to other Pauli-based diagnostics such as Bell magic [56].

Note Added.—During the final stage of this manuscript, we became aware of a related and independent work [84].

Acknowledgement.— Z.X. thanks the helpful discussion with David Huse, Sarang Gopalakrishnan, and Shuo Liu. Z.X. is pleased to acknowledge that the work reported on in this paper was substantially performed using the Princeton Research Computing resources at Princeton University.

* zyxiao@princeton.edu

- [1] P. W. Shor, Polynomial-Time Algorithms for Prime Factorization and Discrete Logarithms on a Quantum Computer, SIAM J. Comput. **26**, 1484 (1997).
- [2] A. M. Childs and W. Van Dam, Quantum algorithms for algebraic problems, Rev. Mod. Phys. **82**, 1 (2010).
- [3] L. Amico, R. Fazio, A. Osterloh, and V. Vedral, Entanglement in many-body systems, Rev. Mod. Phys. **80**, 517 (2008).
- [4] J. Eisert, M. Cramer, and M. B. Plenio, Colloquium:

- Area laws for the entanglement entropy, Rev. Mod. Phys. **82**, 277 (2010).
- [5] J. I. Cirac and P. Zoller, Goals and opportunities in quantum simulation, Nature Phys **8**, 264 (2012).
- [6] M. A. Nielsen and I. L. Chuang, *Quantum Computation and Quantum Information: 10th Anniversary Edition* (Cambridge University Press, 2010).
- [7] S. Aaronson and D. Gottesman, Improved simulation of stabilizer circuits, Phys. Rev. A **70**, 052328 (2004).
- [8] D. Gottesman, The Heisenberg Representation of Quantum Computers (1998), arXiv:quant-ph/9807006.
- [9] S. Bravyi and A. Kitaev, Universal quantum computation with ideal Clifford gates and noisy ancillas, Phys. Rev. A **71**, 022316 (2005).
- [10] M. Howard, J. Wallman, V. Veitch, and J. Emerson, Contextuality supplies the ‘magic’ for quantum computation, Nature **510**, 351 (2014).
- [11] V. Veitch, S. A. Hamed Mousavian, D. Gottesman, and J. Emerson, The resource theory of stabilizer quantum computation, New J. Phys. **16**, 013009 (2014).
- [12] E. Chitambar and G. Gour, Quantum resource theories, Rev. Mod. Phys. **91**, 025001 (2019).
- [13] X. Wang, M. M. Wilde, and Y. Su, Efficiently Computable Bounds for Magic State Distillation, Phys. Rev. Lett. **124**, 090505 (2020).
- [14] Z.-W. Liu and A. Winter, Many-Body Quantum Magic, PRX Quantum **3**, 020333 (2022).
- [15] G. E. Fux, E. Tirrito, M. Dalmonte, and R. Fazio, Entanglement – nonstabilizerness separation in hybrid quantum circuits, Phys. Rev. Research **6**, L042030 (2024).
- [16] M. Bejan, C. McLauchlan, and B. Béria, Dynamical Magic Transitions in Monitored Clifford+ T Circuits, PRX Quantum **5**, 030332 (2024).
- [17] Y. Zhang and Y. Gu, Quantum magic dynamics in random circuits (2024), arXiv:2410.21128 [quant-ph].
- [18] X. Turkeshi, E. Tirrito, and P. Sierant, Magic spreading in random quantum circuits, Nat Commun **16**, 2575 (2025).
- [19] R. Smith, Z. Papić, and A. Hallam, Nonstabilizerness in kinetically constrained Rydberg atom arrays, Phys. Rev. B **111**, 245148 (2025).
- [20] J. Odavić, T. Haug, G. Torre, A. Hamma, F. Franchini, and S. M. Giampaolo, Complexity of frustration: A new source of non-local non-stabilizerness, SciPost Phys. **15**, 131 (2023).
- [21] G. Lami, T. Haug, and J. De Nardis, Quantum State Designs with Clifford-Enhanced Matrix Product States, PRX Quantum **6**, 010345 (2025).
- [22] P. R. N. Falcão, P. Sierant, J. Zakrzewski, and E. Tirrito, Nonstabilizerness Dynamics in Many-Body Localized Systems, Phys. Rev. Lett. **135**, 240404 (2025).
- [23] S. Aditya, X. Turkeshi, and P. Sierant, Growth and spreading of quantum resources under random circuit dynamics (2025), arXiv:2512.14827 [quant-ph].
- [24] S. Aditya, A. Summer, P. Sierant, and X. Turkeshi, Mpemba Effects in Quantum Complexity (2025), arXiv:2509.22176 [quant-ph].
- [25] N. Dowling, P. Kos, and X. Turkeshi, Magic Resources of the Heisenberg Picture, Phys. Rev. Lett. **135**, 050401 (2025).
- [26] Z.-Y. Hou, C. Cao, and Z.-C. Yang, Stabilizer Entanglement Enhances Magic Injection (2025), arXiv:2503.20873 [quant-ph].
- [27] S. Maity and R. Hamazaki, Local spreading of stabilizer Rényi entropy in a brickwork random Clifford circuit (2025), arXiv:2511.07769 [quant-ph].
- [28] D. Szombathy, A. Valli, C. P. Moca, L. Farkas, and G. Zaránd, Independent stabilizer Rényi entropy and entanglement fluctuations in random unitary circuits (2025), arXiv:2501.11489 [quant-ph].
- [29] D. Sticlet, B. Dóra, D. Szombathy, G. Zaránd, and C. P. Moca, Nonstabilizerness in open XXZ spin chains: Universal scaling and dynamics, Phys. Rev. Research **7**, 043130 (2025).
- [30] G. Passarelli, A. Russomanno, and P. Lucignano, Nonstabilizerness of a Boundary Time Crystal, Phys. Rev. A **111**, 062417 (2025), arXiv:2503.05243 [quant-ph].
- [31] B. Magni, A. Christopoulos, A. De Luca, and X. Turkeshi, Anticoncentration in Clifford Circuits and Beyond: From Random Tensor Networks to Pseudomagic States, Phys. Rev. X **15**, 031071 (2025).
- [32] K. Aziz, H. Pan, M. J. Gullans, and J. H. Pixley, Classical Simulations of Low Magic Quantum Dynamics (2025), arXiv:2508.20252 [quant-ph].
- [33] P. S. Tarabunga and E. Tirrito, Magic transition in measurement-only circuits, npj Quantum Inf **11**, 166 (2025).
- [34] D. A. Korbany, M. J. Gullans, and L. Piroli, Long-Range Nonstabilizerness and Phases of Matter, Phys. Rev. Lett. **135**, 160404 (2025).
- [35] G. C. Santra, A. Windey, S. Bandyopadhyay, A. Legramandi, and P. Hauke, Complexity transitions in chaotic quantum systems: Nonstabilizerness, entanglement, and fractal dimension in SYK and random matrix models (2025), arXiv:2505.09707 [quant-ph].
- [36] T. Haug, L. Aolita, and M. S. Kim, Probing quantum complexity via universal saturation of stabilizer entropies, Quantum **9**, 1801 (2025), arXiv:2406.04190 [quant-ph].
- [37] S. F. E. Oliviero, L. Leone, and A. Hamma, Magic-state resource theory for the ground state of the transverse-field Ising model, Phys. Rev. A **106**, 042426 (2022).
- [38] P. S. Tarabunga, Critical behaviors of non-stabilizerness in quantum spin chains, Quantum **8**, 1413 (2024), arXiv:2309.00676 [quant-ph].
- [39] P. R. N. Falcão, P. S. Tarabunga, M. Frau, E. Tirrito, J. Zakrzewski, and M. Dalmonte, Nonstabilizerness in U(1) lattice gauge theory, Phys. Rev. B **111**, L081102 (2025).
- [40] C. D. White, C. Cao, and B. Swingle, Conformal field theories are magical, Phys. Rev. B **103**, 075145 (2021).
- [41] D. Qian and J. Wang, Quantum nonlocal nonstabilizerness, Phys. Rev. A **111**, 052443 (2025).
- [42] M. Frau, P. S. Tarabunga, M. Collura, E. Tirrito, and M. Dalmonte, Stabilizer disentangling of conformal field theories, SciPost Phys. **18**, 165 (2025).
- [43] M. Hoshino, M. Oshikawa, and Y. Ashida, Stabilizer Rényi Entropy and Conformal Field Theory (2025), arXiv:2503.13599 [quant-ph].
- [44] L. Leone, S. F. E. Oliviero, Y. Zhou, and A. Hamma, Quantum Chaos is Quantum, Quantum **5**, 453 (2021), arXiv:2102.08406 [quant-ph].
- [45] X. Turkeshi, A. Dymarsky, and P. Sierant, Pauli spectrum and nonstabilizerness of typical quantum many-body states, Phys. Rev. B **111**, 054301 (2025).
- [46] B. Jasser, J. Odavić, and A. Hamma, Stabilizer entropy and entanglement complexity in the Sachdev-Ye-Kitaev model, Phys. Rev. B **112**, 174204 (2025).

- [47] P. Zhang, S. Zhou, and N. Sun, Stabilizer Rényi Entropy and its Transition in the Coupled Sachdev-Ye-Kitaev Model (2025), arXiv:2509.17417 [quant-ph].
- [48] S. Bera and M. Schirò, Non-Stabilizerness of Sachdev-Ye-Kitaev Model, *SciPost Phys.* **19**, 159 (2025), arXiv:2502.01582 [quant-ph].
- [49] E. Tirrito, X. Turkeshi, and P. Sierant, Anticoncentration and Nonstabilizerness Spreading under Ergodic Quantum Dynamics, *Phys. Rev. Lett.* **135**, 220401 (2025).
- [50] J. Odavić, M. Viscardi, and A. Hamma, Stabilizer entropy in nonintegrable quantum evolutions, *Phys. Rev. B* **112**, 104301 (2025).
- [51] R. Nandkishore and D. A. Huse, Many-Body Localization and Thermalization in Quantum Statistical Mechanics, *Annu. Rev. Condens. Matter Phys.* **6**, 15 (2015).
- [52] M. Beverland, E. Campbell, M. Howard, and V. Kliuchnikov, Lower bounds on the non-Clifford resources for quantum computations, *Quantum Sci. Technol.* **5**, 035009 (2020).
- [53] L. Leone, S. F. E. Oliviero, and A. Hamma, Stabilizer R\'enyi Entropy, *Phys. Rev. Lett.* **128**, 050402 (2022).
- [54] M. Beverland, E. Campbell, M. Howard, and V. Kliuchnikov, Lower bounds on the non-Clifford resources for quantum computations, *Quantum Sci. Technol.* **5**, 035009 (2020).
- [55] J. Jiang and X. Wang, Lower Bound for the \\$T\\$ Count Via Unitary Stabilizer Nullity, *Phys. Rev. Appl.* **19**, 034052 (2023).
- [56] T. Haug and M. Kim, Scalable Measures of Magic Resource for Quantum Computers, *PRX Quantum* **4**, 010301 (2023).
- [57] G. Lami and M. Collura, Unveiling the Stabilizer Group of a Matrix Product State, *Phys. Rev. Lett.* **133**, 010602 (2024).
- [58] L. Chen, R. J. Garcia, K. Bu, and A. Jaffe, Magic of random matrix product states, *Phys. Rev. B* **109**, 174207 (2024).
- [59] T. Haug and L. Piroli, Quantifying nonstabilizerness of matrix product states, *Phys. Rev. B* **107**, 035148 (2023).
- [60] P. S. Tarabunga, E. Tirrito, M. C. Bañuls, and M. Dalmonte, Nonstabilizerness via Matrix Product States in the Pauli Basis, *Phys. Rev. Lett.* **133**, 010601 (2024).
- [61] G. Lami and M. Collura, Nonstabilizerness via Perfect Pauli Sampling of Matrix Product States, *Phys. Rev. Lett.* **131**, 180401 (2023).
- [62] M. Collura, J. D. Nardis, V. Alba, and G. Lami, The non-stabilizerness of fermionic Gaussian states (2025), arXiv:2412.05367 [quant-ph].
- [63] C. Wang, Z.-C. Yang, T. Zhou, and X. Chen, Magic transition in monitored free fermion dynamics (2025), arXiv:2507.10688 [quant-ph].
- [64] Y.-M. Ding, Z. Wang, and Z. Yan, Evaluating Many-Body Stabilizer Rényi Entropy by Sampling Reduced Pauli Strings: Singularities, Volume Law, and Nonlocal Magic, *PRX Quantum* **6**, 030328 (2025).
- [65] Z. Liu and B. K. Clark, Nonequilibrium quantum Monte Carlo algorithm for stabilizer R\'enyi entropy in spin systems, *Phys. Rev. B* **111**, 085144 (2025).
- [66] J. Shanks, Computation of the Fast Walsh-Fourier Transform, *IEEE Trans. Comput.* **C-18**, 457 (1969).
- [67] T. Haug and L. Piroli, Stabilizer entropies and nonstabilizerness monotones, *Quantum* **7**, 1092 (2023).
- [68] L. Leone and L. Bittel, Stabilizer entropies are monotones for magic-state resource theory, *Phys. Rev. A* **110**, L040403 (2024).
- [69] J. L. Walsh, A Closed Set of Normal Orthogonal Functions, *Am. J. Math.* **45**, 5 (1923), 2387224.
- [70] See the Supplemental Material for: (i) the analytic large- N_C behavior of M_2 for $T^{\otimes N}|\psi(N_C)\rangle$; (ii) the special treatment of the identity Pauli string in Monte Carlo sampling; and (iii) the extension of the FWHT framework to subsystem (mixed-state) stabilizer Rényi entropies.
- [71] A. D. Córcoles, J. M. Gambetta, J. M. Chow, J. A. Smolin, M. Ware, J. Strand, B. L. T. Plourde, and M. Steffen, Process verification of two-qubit quantum gates by randomized benchmarking, *Phys. Rev. A* **87**, 030301 (2013).
- [72] A. Nahum, J. Ruhman, S. Vijay, and J. Haah, Quantum Entanglement Growth under Random Unitary Dynamics, *Phys. Rev. X* **7**, 031016 (2017).
- [73] A. Nahum, S. Vijay, and J. Haah, Operator Spreading in Random Unitary Circuits, *Phys. Rev. X* **8**, 021014 (2018).
- [74] N. Metropolis, A. W. Rosenbluth, M. N. Rosenbluth, A. H. Teller, and E. Teller, Equation of State Calculations by Fast Computing Machines, *J. Chem. Phys.* **21**, 1087 (1953).
- [75] W. K. Hastings, Monte Carlo sampling methods using Markov chains and their applications, *Biometrika* **57**, 97 (1970).
- [76] S. Zhou, Z. Yang, A. Hamma, and C. Chamon, Single T gate in a Clifford circuit drives transition to universal entanglement spectrum statistics, *SciPost Phys.* **9**, 087 (2020).
- [77] D. Szombathy, A. Valli, C. P. Moca, J. Asbóth, L. Farkas, T. Rakovszky, and G. Zaránd, Spectral Properties Versus Magic Generation in \\$T\\$-doped Random Clifford Circuits (2025), arXiv:2412.15912 [quant-ph].
- [78] N. D. Varikuti, S. Bandyopadhyay, and P. Hauke, Impact of Clifford operations on non-stabilizing power and quantum chaos (2025), arXiv:2505.14793 [quant-ph].
- [79] Y. Zhang, S. Vijay, Y. Gu, and Y. Bao, Designs from magic-augmented Clifford circuits (2025), arXiv:2507.02828 [quant-ph].
- [80] T. Rakovszky, F. Pollmann, and C. W. Von Keyserlingk, Diffusive Hydrodynamics of Out-of-Time-Ordered Correlators with Charge Conservation, *Phys. Rev. X* **8**, 031058 (2018).
- [81] T. Rakovszky, F. Pollmann, and C. W. von Keyserlingk, Sub-ballistic growth of Rényi entropies due to diffusion, *Phys. Rev. Lett.* **122**, 250602 (2019), arXiv:1901.10502 [cond-mat].
- [82] T. Zhou and A. W. W. Ludwig, Diffusive scaling of Rényi entanglement entropy, *Phys. Rev. Research* **2**, 033020 (2020).
- [83] Z. Lan, M. Van Horssen, S. Powell, and J. P. Garrahan, Quantum Slow Relaxation and Metastability due to Dynamical Constraints, *Phys. Rev. Lett.* **121**, 040603 (2018).
- [84] X. Huang, H.-Z. Li, and J.-X. Zhong, A fast and exact algorithm for stabilizer Rényi entropy via XOR-FWHT (2025), arXiv:2512.24685 [quant-ph].